Journal of Cleaner Production 316 (2021) 128229

Contents lists available at ScienceDirect

Journal of Cleaner Production

journal homepage: www.elsevier.com/locate/jclepro

Life cycle assessment of H_2-selective Pd membranes fabricated by electroless pore-plating

D. Martinez-Diaz [a], P. Leo [b], R. Sanz [b], A. Carrero [a], J.A. Calles [a], D. Alique [a,*]

[a] Department of Chemical, Energy and Mechanical Technology, Rey Juan Carlos University, Móstoles, Spain
[b] Department of Chemical and Environmental Technology, Rey Juan Carlos University, Móstoles, Spain

ARTICLE INFO

Handling Editor: Panos Seferlis

Keywords:
Membrane synthesis
Laboratory-scale
Electroless plating
Palladium
Life cycle assessment
Environmental impacts

ABSTRACT

Pd-based membranes are attracting great attention to reach ultra-pure hydrogen in independent separators or combined with catalysts in membrane reactors. Many advances have been proposed for their fabrication over the last few years, reaching relatively thin Pd-films onto porous substrates with high permeation capacities and mechanical stability, although their commercialization and penetration in the industry are still scarce. At this point, it is important to complete all these technological advances with data about related economic and environmental implications during their fabrication to detect possible bottlenecks and select the best strategy. In this context, the current study presents for the first time a life cycle assessment focused on the preparation of Pd-based composite-membranes by Electroless Pore-Plating (ELP-PP). Two different types of composite membranes supported onto porous stainless steel tubes are analyzed, including or not an additional CeO_2 intermediate layer between the support and the Pd-film. Precise experimental data of the fabrication process at laboratory-scale were considered to account for both materials and energy requirements. Thereafter, the environmental impacts were estimated through ReCiPe methodology by using the software Simapro 8.5. The results evidence that climate change (CC), human toxicity (HT), acidification (AC), freshwater ecotoxicity (FWE), metal depletion (MD) and fossil fuel resources depletion (FD) are the most relevant environmental impacts generated during the manufacturing of the Pd-based membrane. Under this perspective, palladium deposition appears as the manufacturing step with the highest impacts. It can be explained by the metal consumption and the high-energy consumption required for deposition cycles. Thus, the electricity mix of the country where the factory is located is critical to minimize the environmental impacts. For this reason, European countries are expected to be the most favorable ones for membrane fabrication. Finally, comparing both membrane types (with or without a CeO_2 intermediate layer), it can be stated that the incorporation of the ceramic layer noticeably reduces the necessary amount of Pd to reach a fully dense membrane and therefore the associated environmental impacts.

1. Introduction

The current energy system is mainly supported by fossil fuels, responsible for most anthropogenic CO_2 and NOx emissions that provoke serious environmental concerns (YUE and GAO, 2018; Muradov, 2008). The continuous population and economic growth have been made this situation progressively worse during the last decades (Cai et al., 2018; Chen et al., 2016). Only external factors and the natural economic cycles have been slightly modified the velocity of this general trend. For example, the recent world pandemic caused by COVID-19 negatively affects industrial and domestic energy demands, resulting in a marked decrease in atmospheric pollutant levels for many regions worldwide (Aktar et al., 2021; Jiang et al., 2021; Abu-Rayash and Dincer, 2020; Sovacool et al., 2020). Moreover, the numerous international mobility restrictions also significantly influence the restrained energy demand for the transport sector (Corpus-Mendoza et al., 2021). However, it is foreseen this circumstantial situation changes in a few months/years, and the above-mentioned growth's footsteps will be recovered with all its associated environmental implications (Corpus--Mendoza et al., 2021; Szulejko et al., 2017).

In this context, strong policies with a clear roadmap towards a new energy system are fundamental for promoting future sustainability. In fact, diverse regions such as Europe and Japan bet on a progressive transition to renewable energies with very ambitious policies and

* Corresponding author.
E-mail address: david.alique@urjc.es (D. Alique).

https://doi.org/10.1016/j.jclepro.2021.128229
Received 5 February 2021; Received in revised form 1 July 2021; Accepted 4 July 2021
Available online 6 July 2021

important investments to develop new technologies and increase their efficiency (Saeedmanesh et al., 2018; Furlan and Mortarino, 2018). As a clean energy vector, hydrogen is one of the most promising alternatives to facilitate the above-mentioned progressive transition towards a net-zero carbon emissions system (Parra et al., 2019). In this context, new ambitious policies try to promote this technology in Europe during next years (Lux and Pfluger, 2020; Kakoulaki et al., 2021), following the first steps recently taken by Japan (Pambudi et al., 2017; Ozawa et al., 2018). Among other multiple reasons, the possibility to be produced from a wide variety of feedstock by diverse technologies, some of them very mature, could definitively promote its penetration in the industry with assumable risks (Baykara, 2018). In fact, most of the current hydrogen is produced by methane steam reforming (Choi et al., 2016; Coutanceau et al., 2018; Kim et al., 2017), although many other hydrocarbons can also be considered with similar technologies. The use of biomass-derivate compounds and wastes to generate hydrogen could be especially attractive for a circular economy (Baykara, 2018; Detchusananard et al., 2018; Yin and Yip, 2017). However, in all these processes involving traditional thermochemical routes, hydrogen is not directly obtained in its pure form but accompanied by other sub-products such as carbon monoxide, carbon dioxide, methane, or steam water, among others (Baykara, 2018; Nikolaidis and Poullikkas, 2017). Therefore, down-stream additional purification steps are always required to adjust the hydrogen purity for each particular final application (Zornoza et al., 2013; Bernardo et al., 2020). In this context, it is important to point out that the overall economy of the production processes is significantly affected by these purification steps, reaching up to 50% of the total cost in function of the selected technology and operating conditions (Sholl, 2016). Pressure swing adsorption (PSA) is currently the prevalent alternative for hydrogen purification in most industrial processes, despite its high energy consumption and limited profitability for small production-scale as suggested by a decentralized energy system (Wim Elseviers et al., 2015; Mivechian and Pakizeh, 2013; Voss, 2005). Many researchers have also promoted the use of H_2-selective membranes for this purpose during the last years (Alique et al., 2018a). This alternative provides the possibility to reach an ultra-high purity in a wide variety of operating conditions, including the combination of both production and separation steps in a unique device so-called membrane reactor (Brunetti et al., 2017; Liguori et al., 2020). The continuous separation of hydrogen throughout the membrane from the bulk reaction promotes its generation by an equilibrium displacement towards the products (Cao et al., 2012). This technology simultaneously aims to facilitate the process intensification and increase their overall efficiency (Gallucci et al., 2013; Karagöz et al., 2020).

Among the various membranes used in the devices mentioned above, those dense ones made of pure palladium or its alloys provide clear advantages in terms of H_2 perm-selectivity and mechanical resistance at high temperatures (Arratibel Plazaola et al., 2017; Conde et al., 2017). Hydrogen permeation through these metal dense-membranes is typically expressed by the Sieverts' law, defined as follows:

$$J_{H_2} = \frac{\mathscr{P}}{t_{Pd}} \left[{p_{H_2,ret}}^{0.5} - {p_{H_2,perm}}^{0.5} \right] = \mathscr{P}^* \left[{p_{H_2,\,ret}}^{0.5} - {p_{H_2,\,perm}}^{0.5} \right] \quad \text{(Eq. 1)}$$

where J_{H2} is the permeate flux (mol m^{-2} s^{-1}), $\mathscr{P}$ the H_2 permeability (mol m^{-1} s^{-1} $Pa^{-0.5}$), $\mathscr{P}^*$ the H_2 permeance (mol m^{-2} s^{-1} $Pa^{-0.5}$), t_{Pd} the thickness of the Pd-based layer (m^{-1}) and $p_{H2,i}$ (Pa) the hydrogen partial pressure in both retentate (subscript $i = ret$) and permeate (subscript $i = perm$) sides.

In this manner, the hydrogen flux through a Pd-based membrane depends on some operating conditions and intrinsic membrane properties. The pressure difference between both retentate and permeate side is the first group's most relevant one together with the temperature, which affects the membrane permeability by an Arrhenius-type dependence (Calles et al., 2014). On the other side, the membrane composition and the metal thickness are the second group's most relevant ones (Yun et al., 2011; Tarditi et al., 2017). They should be considered in any membrane fabrication strategy for their final commercialization. In this context, great efforts are being carried out during last years to reduce as much as possible the metal thickness of these membranes, reaching values below 15 μm by incorporating the Pd-film onto porous supports that provide the required mechanical resistance (Melendez et al., 2017). Among all the porous materials that can be used as membrane support, alumina and stainless steel are the most prevalent ones in the literature. The first ones provide a very smooth surface with small pores and narrow pore-size distribution that eventually makes the Pd-incorporation easier, although the material is relatively weak for handling and their thermal expansion coefficient is quite different to the palladium, thus being possible to generate stress under thermal cycles. On the contrary, the stainless steel supports offer high mechanical resistance to handle and a thermal expansion coefficient very close to that of the palladium film, thus ensuring the lifespan of composite-membranes despite suffering thermal stress. However, their morphological surface properties are less favorable to reach ultra-thin Pd-film without further modifications (Alique et al., 2016, 2018b). In this context, each author bet on one particular alternative based on their particular interests. Electroless Plating (ELP) and its variants have demonstrated a great potential to achieve these goals onto porous supports of diverse nature and geometry with contained expenses (Dogan and Kilicarslan, 2008; Souleimanova et al., 2000; M, 1990). Particularly, the Electroless Pore-Plating (ELP-PP) alternative offers an excellent adherence of the Pd-film onto the porous support and, hence, a high mechanical resistance of resulting composite-membranes even in case of generating tensile stress during their operation (Alique et al., 2020; Tosto et al., 2020). It is reached thanks to a partial palladium infiltration into some pores after placing both Pd-source and hydrazine solution, the reducing agent, from opposite sides of the support (Alique et al., 2018a; Sanz et al., 2012).

Moreover, an intermediate layer between the porous support and the top Pd-film is frequently included to reduce both original roughness and average pore sizes and, consequently, make the generation of thin Pd layers easier (Yepes et al., 2006; Mateos-Pedrero et al., 2010; Zheng et al., 2016). A wide variety of materials have been proposed as interlayers, highlighting technical ceramics such as alumina (Bottino et al., 2014), zirconia (Hatlevik et al., 2010), yttria-stabilized zirconia (Han et al., 2017; Huang and Dittmeyer, 2007; Sanz et al., 2011), or ceria (Martinez-Diaz et al., 2019, 2020; Ryi et al., 2014), among others. These materials have also been used as an additional fourth layer onto the H_2-selective Pd-film for protection against the particular operating conditions of fluidized-bed reactors (Arratibel et al., 2018a, 2018b). Most of these fabrication strategies are developed to improve the final performance of the membrane in terms of permeation capacity and mechanical stability. However, reports about economic or environmental implications are certainly scarce even though these implications are critical issues for commercializing the membranes and their penetration in the industry. In this sense, the use of Life Cycle Assessments (LCA) is extended as an accurate technique to quantify the environmental impacts generated by processes or products rigorously (Simonen, 2014). This methodology allows a systematic estimation of the environmental changes caused during the fabrication of a certain material or a process itself. Basically, it consists of examining all processes involved in the case under study, quantifying all material and energy inputs/outputs to determine their effects on both human health and the environment according to a standardized procedure described in ISO-14040 and ISO-14044 (Finkbeiner et al., 2006). In this context, LCA has proved to be a useful tool for the assessment of environmental impacts in the energy and fuel sector (Turconi et al., 2013; Igos et al., 2015). Despite this fact, the environmental studies focused on hydrogen production processes containing Pd-based membranes are really scarce in the specialized literature. Di Marcobernardino et al. analyzed the environmental and economic performances of an innovative micro-CHP system based on a membrane-reactor and a PEM fuel-cell (Di Marcoberardino et al., 2017). The results were compared with an analogous

system in which the hydrogen is produced in a traditional steam reformer for diverse scenarios. They evidenced that the innovative system based on a membrane-reactor reduces or has similar impacts for the carbon footprint depending on the assumed scenarios. Simultaneously, water withdrawal and human health were positive or negative, depending on the case. However, almost no references about the analysis of environmental impacts produced during the synthesis of inorganic membranes can be found in the literature. For instance, it is possible to find some punctual study about the environmental evaluation of zeolite membrane manufacturing by LCA (Navajas et al., 2018) but, to the best of our knowledge, no available studies include Pd-based membranes. This work tries to cover this gap, including for the first time a systematic environmental analysis throughout LCA to fabricate, at laboratory-scale, Electroless Pore-Plated composite-membranes onto PSS supports. Previous results evidenced the clear benefits of incorporating CeO_2 intermediate layers between the porous substrate and the H_2-selective film to reduce its thickness up to around 15 μm, and hence its overall preparation cost while increasing its the hydrogen flux around 400% about previous results in which no ceramic intermediate layers were considered. In this manner, H_2-permeance of $5.37{\cdot}10^{-4}$ mol m^{-2} s^{-1} $Pa^{-0.5}$ was reached at 400 °C with an ideal H_2/N_2 perm-selectivity ≥10000 and activation energy of 8.9 kJ mol^{-1} (Martinez-Diaz et al., 2019). In the present study, the overall environmental impacts generated during the synthesis of these ELP-PP Pd-membranes, considering or not the use of a ceramic barrier of CeO_2 between the PSS support and the Pd-film, are presented to complete the previous technical insights and select the best strategy for their fabrication. Besides the most relevant results that concern the environmental impacts, including a discussion about the possible location of the factory, the main uncertainties and possible limitations of the study have been also addressed. In this manner, the present contribution could provide a new tool to select the most favorable strategy for the synthesis of Pd-based membranes in terms of both technical and environmental aspects.

2. Experimental section

2.1. Membrane preparation

All composite-membranes considered in this work were prepared onto commercial AISI 316L porous stainless-steel (PSS) supports with cylindrical geometry purchased from Mott Metallurgical corp. The original tubes present symmetric structure with 0.1 μm porous media grade, an external diameter of 12.7 mm and around 2.0 mm wall thickness, within the typical values of porous supports conventionally used for the preparation of H_2-selective membranes. These tubes were cut into smaller lengths of around 30 mm for preparing each composite-membrane at laboratory-scale as described in previous studies (Martinez-Diaz et al., 2019, 2020, 2021). In this context, it should be pointed out that considering the above-mentioned dimensions, the effective permeation area for each particular application is usually reached by fitting both the length and the number of tubes.

Two different composite-structures containing various intermediate layers were considered for the analysis, as illustrated in Fig. 1.

In both cases, the raw PSS supports were first calcined in air to generate an initial thin intermediate layer made of Fe–Cr oxides according to a previous investigation (Furones and Alique, 2017; Maroño et al., 2020). One of these samples, denoted as MB#01, was directly used to incorporate the top H_2-selective film made of pure palladium by Electroless Pore-Plating (ELP-PP) following the procedure described elsewhere (Sanz et al., 2012; Calles et al., 2018). On the other hand, an additional intermediate layer formed by dense cerium oxide particles was incorporated by vacuum-assisted dip-coating in the sample MB#02 before the top Pd-film (Martinez-Diaz et al., 2019).

Fig. 2 summarizes a detailed scheme of the synthesis procedure followed for each membrane. Basically, all steps can be divided into two main groups: Support Modification (SM) and Palladium Deposition (PD). The first one, SM, consists of an initial cleaning of raw PSS supports to remove eventual dirty or grease from their manipulation (SM-1) and the incorporation of intermediate layers (Fe–Cr oxides and CeO_2) to modify the original surface supports (SM-2 to SM-4). The second one, PD, includes the activation of the modified surface with homogeneously

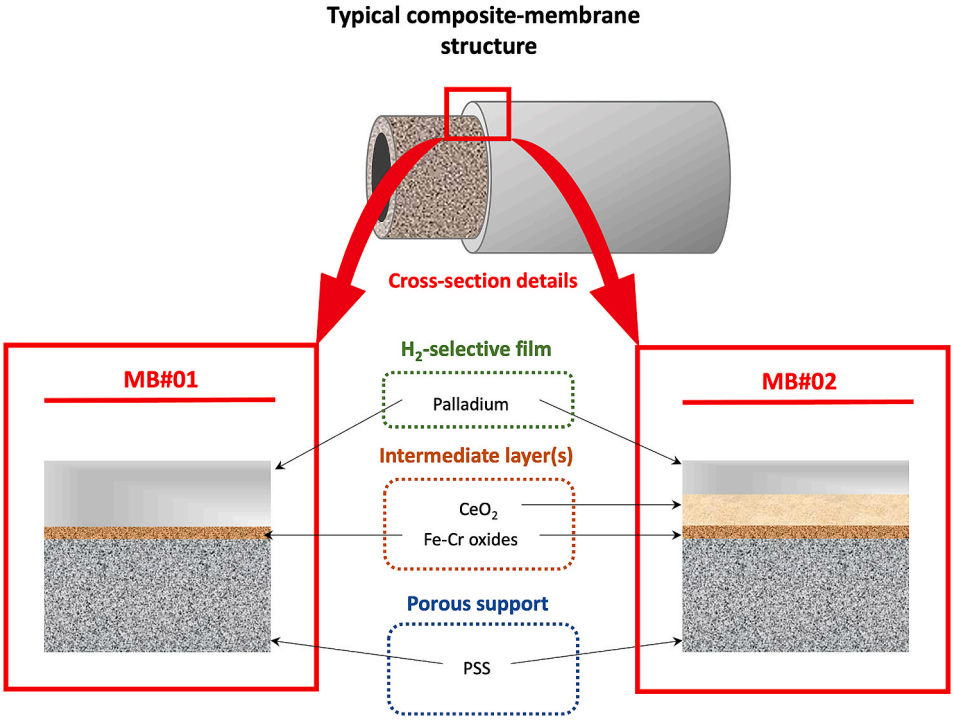

Fig. 1. Schematic composite-structures of Pd-membranes considered in the present study.

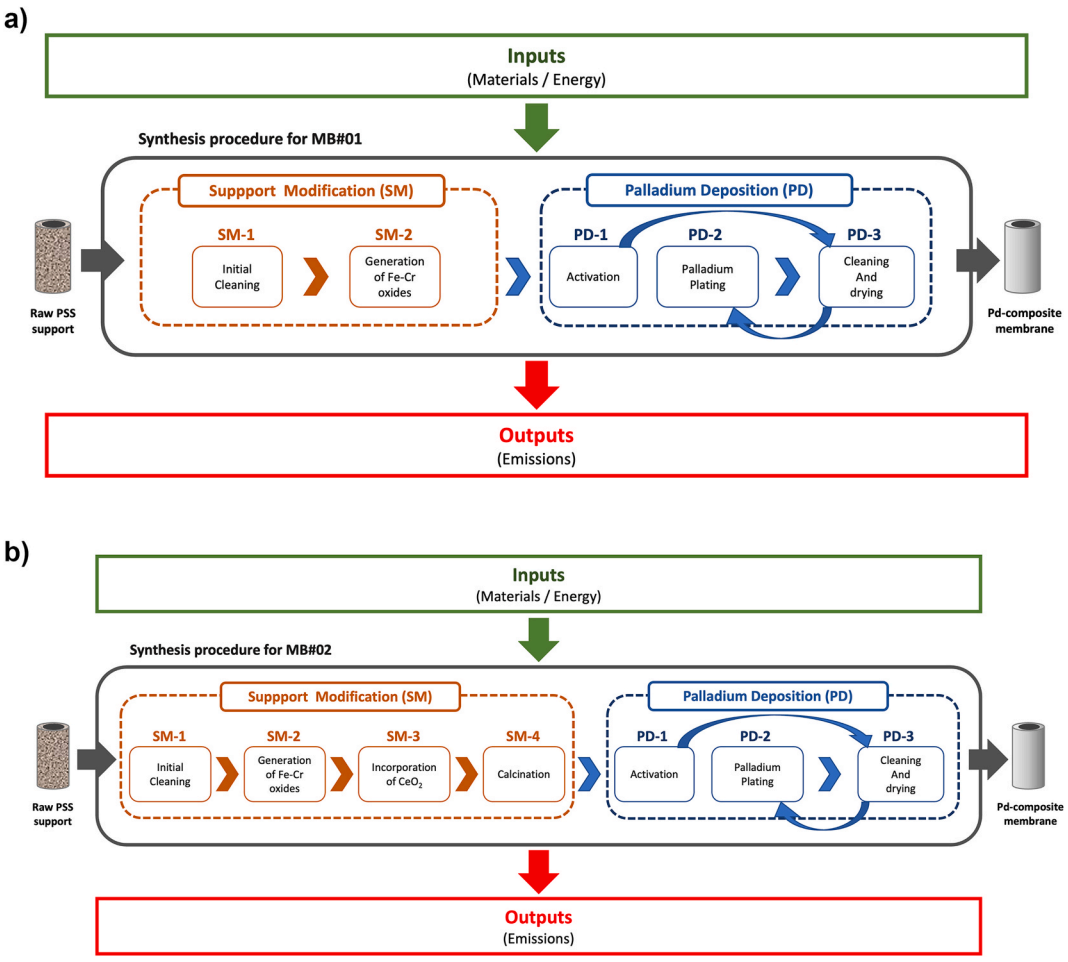

Fig. 2. Detailed scheme of the synthesis procedure followed for: a) MB#01 and b) MB#02.

distributed fine Pd-nuclei (PD-1), the incorporation of the fully dense Pd-film by ELP-PP (PD-2), and the required cleaning and drying steps after both steps (PD-3). At this point, it should be noted that the last steps were repeated several times up to reach complete gas tightness, thus evidencing a good continuity of the Pd-film and absence of detectable defects at room conditions.

All these steps require particular inputs in form of materials and/or energy while generating some eventual output emissions. To a better understanding of these inputs and outputs during the synthesis process of each membrane included in the present work, some additional key information is included here. The first step always consists of cleaning the raw PSS supports by successive immersions in diverse solutions of sodium hydroxide 0.1 M (SM-1.1), hydrochloric acid 0.1 M (SM-1.2), and ethanol 96 vol% (SM-1.3) at 60 °C under ultrasonic stirring. Then, the clean supports were oxidized in air at 600 °C (heating and cooling rams of 1.8 °C/min) for 12 h in a tubular furnace to generate a primary intermediate layer formed by a thin Fe/Cr oxides layer. In previous studies, it was concluded that this thin film slightly reduces the roughness and average pore size of the original PSS supports at the external surface, thus moderately promoting the subsequent incorporation of a Pd-film with reduced thickness by ELP-PP (Furones and Alique, 2017; Maroño et al., 2020).

MB#01 has been prepared directly at these conditions, without considering further modifications of the porous substrate. The palladium deposition by ELP-PP always involves three successive main steps, repeating some of them several times up to achieve a fully dense membrane. Some nano-sized Pd-nuclei need to be finely distributed onto the surface of the pores before initiating the plating. This is to guarantee a homogeneous growth of the film, good adherence, and reasonable induction times to initiate spontaneously the chemical reactions involved in ELP-PP. In this step, denoted as activation, the extremes of the support are sealing with Teflon tapes to maintain separated both external and internal sides from where two different solutions are fed: 0.1 g/l acidic palladium chloride as metal source (PD-1.1) and 0.2 M N_2H_4 – 2.0 M NH_4OH mixture as reducing agent (PD-1.2), respectively. The immersion of the support in the solutions is maintained for 2 h at room temperature, preferentially meeting both PD-1.1 and PD-1.2 solutions just into the pores and initiating the generation of the first Pd-nuclei. After this time, the support is washed in distilled water and dried at 110 °C for at least 8 h before starting the ELP-PP strictly speaking. The Pd plating is then completing in similar conditions but increasing the temperature up to 60 °C and replacing both Pd source and reducing solutions with new ones: PD-2.1 and PD-2.2. The first one, PD-2.1, contains the Pd precursor ($PdCl_2$, 99 w.%) complexed and stabilized with NH_4OH (32 vol%) and Na_2EDTA, while the second one, PD-2.2, includes diluted N_2H_4 in water (0.2 M) as reducing agent. Then, Pd^{2+} ions contained in PD-2.1 are reduced to Pd^0 in a controlled autocatalytic chemical reaction for various cycles of 2–7 h. Intermediate washing in distilled water and dried at 110 °C for at least 8 h are performed between each cycle. This procedure is repeated up to the Pd weight gain of the membrane became negligible due to the complete blockage of pores and, consequently, the achievement of a fully dense Pd-membrane (Alique et al., 2018a, 2018b, 2020).

MB#02 has been prepared following a similar experimental procedure but incorporating an additional CeO_2 intermediate layer as described in a previous study (Martinez-Diaz et al., 2019). It involves

two new steps for the support modification: the incorporation of the material onto the support by vacuum-assisted dip-coating (VA-DC) and its calcination to ensure good stability of the new layer, respectively denoted as SM-3 and SM-4. In particular, commercial dense CeO_2 particles (Alfa-Aesar, 100 nm average particle size) are suspended in water containing 2 wt% polyvinyl alcohol (PVA) to reach a CeO_2 concentration of around 20 wt% (SM-3.1). After sealing the inner side of the support with appropriate Teflon tapes, VA-DC is repeated twice by applying vacuum only during the half-second cycle. The CeO_2 layer thickness is finally adjusted by rinsing in distilled water and then the composite-structure is calcined at 500 °C (heating and cooling ramp of 1.8 °C/min) for 5 h to ensure the complete removal of the organic linker (PVA) and good mechanical stability of the intermediate layer (Martinez-Diaz et al., 2019).

Table 1 summarizes all chemicals and materials used for the preparation of the above-mentioned SM and PD solutions. Besides all these chemicals and materials, the energy requirements of each step need to be also considered in the present study. At this point, it is important to emphasize the laboratory scale of the analyzed membrane synthesis procedures. Thus, the optimization of these issues should be taken into account for the next scale-up considerations. In this context, a different number of membranes can be managed at each particular preparation step. Four membranes can be simultaneously handled in steps SM-1, PD-1, PD-2, and PD-3, while two samples can be processed in steps SM-2 and SM-4 at the same time. Other steps (SM-3 and PD-1) are performed individually for each membrane.

2.2. LCA methodology

The LCA analysis presented in the present study was performed according to standards ISO-14040 and ISO-14044 to determine the effects of each material and energy input/output used in the previously described membranes manufacturing process on both human health and the environment.

2.2.1. LCA goal and scope

The present study is focused on the evaluation of all main environmental impacts and energy demands related to the fabrication of two different supported Pd-based membranes by ELP-PP at a laboratory scale (MB#01 and MB#02). The objective is figuring out the most impacting operations from an energy and environmental point of view to produce these membranes. In this manner, it would be possible to improve the synthesis strategies and/or select the most appropriate one for pilot or pre-industrial scales. A cradle-to-gate perspective was considered to perform the analysis and determine the corresponding inputs and outputs. It implies contemplating all issues required from the acquisition of the raw materials to Pd deposition by ELP-PP, as previously represented in Fig. 2. The cradle starts with the extraction of natural resources (e.g., oil, natural gas, minerals, etc.), while and the gate ends with the output of the functional unit, which means the final ELP-PP Pd-membrane. Later uses and lifespan of Pd-composite membranes are assumed to be relatively independent of the production technology, so they were not considered for the LCA. Moreover, the use of these membranes in both H_2-separators or membrane reactors is an emerging technology so there is no much information about possible end-of-life treatments or recycling processes.

Diverse criteria can be followed to select the most appropriate functional unit for a particular LCA. Membrane technologists usually analyze the experimental performance of materials with particular dimensions in their studies and, based on these results, they predict the foreseeable membrane area to be used in processes with a certain hydrogen capacity. This strategy is also adopted to compare different synthesis alternatives for the membranes based on technical results reached from laboratory or pilot-plant experiments. However, it is clear that both membrane dimensions and fabrication capacity could affect the conclusions extracted from this comparison, especially in the case of taking into account environmental issues. Thus, the synthesis of one simple tubular Pd-membrane with 30 mm in length and 12.7 mm of external diameter was selected as functional unit in this study to have a large data inventory of experimental materials and energy consumption during its preparation and compare the environmental burdens of diverse synthesis strategies.

2.2.2. System boundaries and life cycle inventory

All inputs required for the fabrication of Pd-membranes, including both materials and energy, as well as the generated outputs during the synthesis procedure, were considered within the system boundaries graphically described in Fig. 2. All particular data used for the life cycle inventory was directly obtained from experiments at laboratory scale, including the consumption of reagents and electricity. More details about this inventory can be found in Table S2 and Table S3 as supporting information for the preparation of the membranes MB#01 and MB#02, respectively. Regarding the energy mix, it should be noted that the original conditions available in the Ecoinvent 3.4 database were updated through energy estimates provided by the official public bodies of each country. In fact, specific conditions of five different countries were considered: Spain, Germany, China, Japan, and the United States of America. Table 2 collects the contribution of each primary source to the available energy mix in these countries.

2.2.3. Life cycle impact assessment (LCIA)

In this work, the software Simapro v8.5 was used to assess all environmental impacts by using the inventory data above detailed. The evaluation of environmental impacts related to the process was carried out by using a mid-point methodology. This approach is more precise since mid-points are considered to be bonds in the cause-effect chain (environmental mechanism) of an impact category. On the contrary, characterization factors or indicators taken from an end-point approach

Table 1
Summary of chemical and materials requirements for solutions used during the synthesis of the membranes.

SM: Surface Modification				PD: Palladium Deposition			
SM-1: Initial cleaning		**SM-3: CeO_2 barrier**		**PD-1: Activation**		**PD-2: ELP-PP**	
SM-1.1		**SM-3.1**		**PD-1.1**		**PD-2.1**	
NaOH (g/l)	2	CeO_2 (g/l)	100	$PdCl_2$ (g/l)	0.1	$PdCl_2$ (g/l)	5.4
SM-1.2		PVA (g/l)	20	HCl 35% (ml/l)	1	NH_4OH 32% (ml/l)	390
HCl 35% (ml/l)	2			**PD-1.2**		Na_2EDTA (g/l)	70
SM-1.3				NH4OH 32% (ml/l)	120	**PD-2.2**	
Ethanol 96% (ml/l)	1000			N_2H_4 (ml/l)	10	N_2H_4 (ml/l)	10

Table 2
Energy mix 2019 available in different countries with a particular interest in the present study.

Source	Contribution to the energy mix (%)				
	Spain (SistemaInforme, 2019)	Germany (BDEW and Energieversorgung, 2020)	China (US Energy Information Administration (EIA, (2020))	Japan (Yanagisawa et al., 2014)	USA (EIA, 2020)
Hard coal	4.3	6.4	65.6	32.7	23
Lignite	–	13.5	–	8.7	–
Hydro	10	3.4	17.7	7.9	6.6
Natural gas	32.7	16.1	3.1	39.5	38.8
Nuclear	22.6	11.3	4.8	3.1	20.7
Wind	21.5	26.8	5.5	2.3	7.3
Biomass	–	8.0	0.2	2.7	1.4
Solar	2.1	9.7	3.1	3.1	1.8
Others	6.8	4.8	–	–	0.4

can be calculated to reflect intentionally the relative importance of a particular emission or impact category (Bare et al., 2000; Huijbregts et al., 2017). In this manner, a relatively independent and rigorous overview about the environmental profile reached during the synthesis of Pd-based composite-membranes can be reached, while quantifying a wide variety of environmental effects on multiple impact categories. Under this perspective, the ReCiPe methodology was selected as one of the most adequate hierarchical perspectives since it was also previously applied to other LCA studies for the preparation of inorganic membranes (Prézélus et al., 2021) and diverse hydrogen-production processes (Valente et al., 2017).

All environmental impacts related to each category addressed in the ReCiPe methodology were calculated (complete data in Fig. S1 as supplementary information), although only the most relevant ones were chosen through a contribution analysis to be further discussed: climate change (CC), human toxicity (HT), acidification (AC), freshwater ecotoxicity (FWE), metal depletion (MD) and fossil fuel resources depletion (FD). The rest of the categories, with a minimum single score on the total environmental impact, were excluded. Moreover, the total energy requirements of the process were also quantified through cumulative energy demand (CED) (Huijbregts et al., 2010).

Finally, a Monte-Carlo analysis, carried out for all impact categories, has been also included to analyze the uncertainty of reached results and compare both membrane fabrication strategies. The proposed simulation was done with 1000 runs, while uncertainty values used for the background parameter were based on the uncertainty parameters provided by Ecoinvent 3.4 consequential (Wernet et al., 2016).

3. Results and discussion

3.1. Fundamental membrane characterization

The primary characterization of any composite-membrane always includes the analysis of the morphology variation during the synthesis procedure. As previously addressed, the two different ELP-PP membranes included in the present work were fabricated following a similar strategy with the unique variation of incorporating an additional intermediate layer formed by dense CeO_2 particles (Alique et al., 2020; Martinez-Diaz et al., 2019). Fig. 3 collects some relevant micrographs taken for each membrane to discuss briefly their main characteristics.

As can be seen, a very irregular external surface with a wide variety of pore sizes and high roughness appears in MB#01 despite being

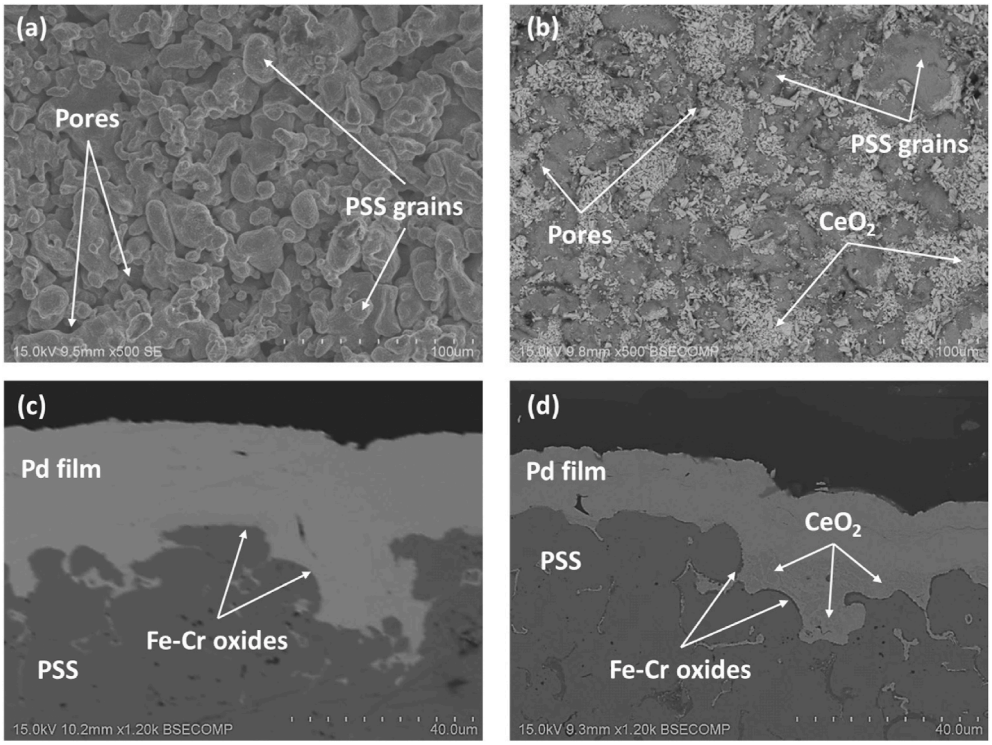

Fig. 3. Morphology of MB#01 and MB#02 membranes before (a and b, respectively) and after incorporating the Pd-film by ELP-PP (c and d, respectively).

oxidized in air to generate a first intermediate layer of Fe–Cr oxides (Fig. 3a). Only after the incorporation of CeO_2 particles in MB#02 was possible to smooth the external surface of supports, significantly reducing the average pore-mouth diameter before the palladium plating (Fig. 3a). The different morphologies reached for each case provoke an important effect on the Pd-film characteristics. In this manner, an estimated Pd-thickness from gravimetric analysis around 28 μm was required to obtain a gas-tightness membrane (MB#01), although it was reduced up to 15 μm in case of including the CeO_2 intermediate layer (MB#02). These values are fairly close to the real Pd-thicknesses directly measured onto the SEM cross-sectional images, as shown in Fig. 3c and d for membranes MB#01 and MB#02, respectively. This relevant improvement can be explained by the generation of a new media grade with smaller pore sizes that can be more easily close by palladium particles during ELP-PP as widely discussed in previous works (Alique et al., 2020; Martinez-Diaz et al., 2019).

As a consequence of the different membrane properties, mainly the final Pd-thickness reached for each case, a marked effect on the membrane performance was observed in terms of permeation capacity. Fig. 4 collects the H_2-permeate fluxes reached at 400 °C for pressures ranged from 0.25 to 2.50 bar when operating with MB#01 and MB#02. At this point, it is important to note that no nitrogen was detected in the permeate during the complete set of experiments (detection limit $1.67{\cdot}10^{-2}$ mL min^{-1}), and therefore, an ideal H_2/N_2 separation factor ($\alpha_{H2/N2}$) greater than 10,000 can be ensured for both samples.

Analyzing in detail for each sample the relationship between H_2 fluxes and pressures raised to the power of 0.5, a clear linear trend is observed, as predicted by the well-known Sieverts' law (Eq. (1)) (Yun et al., 2011; Caravella et al., 2013).

This fact together with the undetectable permeate fluxes in the case of feeding nitrogen confirms the absence of defects in the palladium film previously supposed after the membrane preparation. Thus, H_2-diffusion through the Pd-film can be considered as the rate-determining step, as typically occurs in most of the Pd-composite membranes (Vadrucci et al., 2013; Bellini et al., 2020).

However, it is also clear that the above-mentioned linear trends do not intercept the origin as common in other cases. This peculiar behavior is typical of most ELP-PP membranes reported up to now, being widely addressed in previous studies (Alique et al., 2018a, 2018b, 2020). In essence, this deviation is justified by the partial infiltration of palladium into some pores of the support during the ELP-PP cycles due to feeding both metal source and the reducing agent from opposite sides of the porous substrate. This fact generates noticeably differences between both external and internal surfaces of the Pd-film that affect to the accurate calculation of the pressure driving force just onto the surfaces, as considered in the Sieverts' law (Martinez-Diaz et al., 2021). Pressure values into the bulk gas phase and smooth surfaces are almost identical, thus being possible to precise them with minimal errors. On the contrary, in the case of presenting relevant tortuosity, as typically occurs for ELP-PP Pd-film surfaces in contact with porous supports, relevant pressure drops could appear between the measured pressure value into the bulk gas phase and just onto that palladium side. It can be quantified as an apparent additional resistance against the permeation process (R_i) as detailed in previous works (Alique et al., 2018a, 2018b, 2020). Anyway, the benefits of using an additional CeO_2 intermediate layer in MB#02 becomes obvious in terms of its performance, reaching H_2 permeance of $5.37{\cdot}10^{-4}$ mol m^{-2} s^{-1} $Pa^{-0.5}$ at 400 °C, in contrast to the lower value obtained in MB#01, $1.50{\cdot}10^{-4}$ mol m^{-2} s^{-1} $Pa^{-0.5}$ at analogous conditions. Undeniably, this improvement of the permeation capacity in around 350% is caused by the reduction of the Pd-thickness required to achieve a fully dense membrane in case of using the additional CeO_2 barrier (from 28 to 15 μm, as previously discussed). Table 3 summarizes all these results for easier comparison.

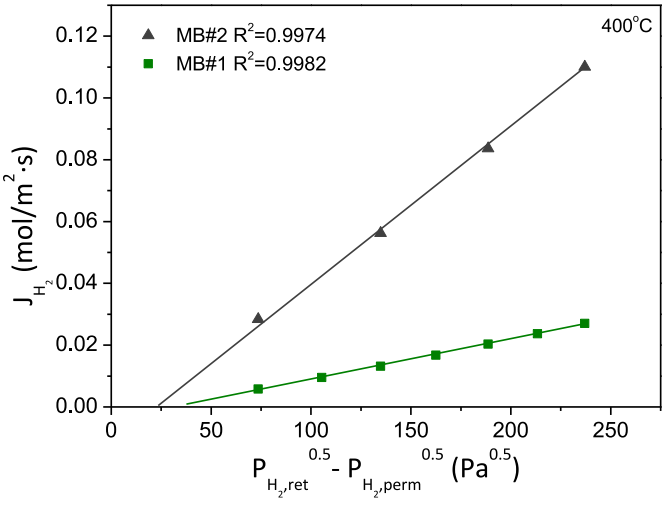

Fig. 4. Permeation behavior of ELP-PP membranes MB#01 and MB#02 at 400 °C.

To compare these results with different available data in literature, the performance of other relevant composite membranes prepared by electroless plating and related techniques have been included in Table 4. Membranes prepared onto both metallic and ceramic supports have been considered for comparison. As can be seen, a wide variety of palladium thicknesses can be found, usually affecting the H_2-permeation. In general, thicker membranes provides a lower permeation capacity but greater selectivity and viceversa. Moreover, it should be noted that a wide variety of dimensions, specially for membrane length, can be found in literature, despite considering tubular geometry in all cases.

3.2. Materials inventory for membranes preparation

Up to now, it is clear the benefits provided by the strategy of using an additional ceramic intermediate layer for the preparation of ELP-PP membranes in terms of palladium savings and final performance. However, no considerations about the environmental impacts of all associated experimental steps have been taken into account. This lack of information is very common in most of the available researches despite it could generate important implications for the commercialization and spread of this technology. This work tries to fill in the gap in this field, providing complete and precise information about all materials required for the preparation of the membranes step by step, particularly those obtained by ELP-PP. At this point, it should be remembered that two different synthesis strategies have been considered for the preparation of these composite-membranes in the present study, including or not an intermediate ceramic barrier formed by CeO_2 particles. Since all the membranes were prepared onto the same tubular PSS supports, its contribution to the environmental impact has been omitted to point out exclusively the considerations of each synthesis procedure.

In this context, Tables 5 and 6 include a complete material inventory for each step carried out for the surface modification (SM) and palladium deposition (PD), respectively, during the preparation of two different types of ELP-PP membranes. At this point, it has to point out that 6 different membranes of each type (similar to MB#01 and MB#02) were fabricated to ensure good reproducibility of the results here collected. The solutions required for modifying the original surface of raw PSS supports (SM) used to prepare the composite membranes accordingly to the procedures previously described are summarized in Table 5. Only the initial cleaning of the supports (SM-1), common for both membranes included in the present study, and the incorporation of the CeO_2 intermediate layer (SM-3), carried out just for MB#02, require the use of chemicals and solutions. However, it should be noted that after each of the above-mentioned cycles the membrane is always rinsed with distilled water, thus requiring an additional water consumption of around 40 mL besides the considered one for the preparation of the aqueous solutions. Moreover, it is important to emphasize that all these

Table 3
Summary of main properties for membranes included in the present study.

Sample	Membrane morphology			Permeation behavior		
	Intermediate layer(s)	t_{Pd} (μm)	Variation (%)	R_i ($Pa^{0.5}$)	$\mathscr{P}^*$ (mol m^{-2} s^{-1} $Pa^{-0.5}$)	Variation (%)
MB#01	Fe–Cr oxides	28	–	24	$1.50{\cdot}10^{-4}$	–
MB#02	Fe–Cr oxides/CeO_2	15	- 46.4%	33	$5.37{\cdot}10^{-4}$	+358%

Table 4
Performance survey for relevant membranes prepared by Electroless Plating and related techniques from the available literature.

Support	Membrane geometry			H_2-selective film			Membrane performance		Ref
	L (mm)	ID (mm)	OD (mm)	Material	t_{Pd} (μm)	T (°C)	$\mathscr{P}^*$ (mol s^{-1} m^{-2} $Pa^{-0.5}$)	$\alpha_{H2/N2}$	
PSS (316L)	36	n.a.	10.0	PdAu	12.0	450	$1.30{\cdot}10^{-3}$	12,400	Anzelmo et al. (2018)
Al_2O_3	48	10.0	14.0	Pd	5.0	400	$6.32{\cdot}10^{-4}$*	9000	Zhao et al. (2018a)
PSS (316L)	250	n.a.	12.7	Pd	7.0	500	$2.26{\cdot}10^{-3}$	145	Kim et al. (2018)
Al_2O_3	50	8.0	13.0	PdAu	8.0	400	$1.80{\cdot}10^{-3}$[a]	500	Iulianelli et al. (2019)
Al_2O_3	75	9.0	10.0	Pd	6.0	500	$1.71{\cdot}10^{-4}$[a]	268	Guo et al. (2017)
PSS	450	n.a.	12.7	Pd	4.5	550	$2.40{\cdot}10^{-3}$	618	Kim et al. (2018)
Al_2O_3	75	8.0	13.0	Pd	5.0	400	$7.28{\cdot}10^{-4}$	2500	Huang et al. (2020)
Al_2O_3	1000	n.a.	14.0	Pd	240.0	450	$2.80{\cdot}10^{-4}$	66,000	Peters et al. (2018)
Al_2O_3	52	10.0	14.0	Pd	6.3	500	$1.48{\cdot}10^{-3}$[a]	4832	Zhao et al. (2018b)
PSS (316L)	30	9.0	12.7	Pd	28.0	400	$1.50{\cdot}10^{-4}$	≥10,000	This work
PSS (316L)	30	9.0	12.7	Pd	15.0	400	$5.37{\cdot}10^{-4}$	≥10,000	This work

n.a. = non-available data.
[a] Calculated from available published data in the work.

Table 5
Materials inventory for surface modification of PSS supports during membrane preparation (referred to the selected functional unit).

Sample	Solutions required for surface modification (SM)									
	SM-1						SM-2	SM-3		SM-4
	SM-1.1		SM-1.2		SM-1.3			SM-3.1		
	Cycles	**V (mL)**	**cycles**	**V (mL)**	**cycles**	**V (mL)**		**cycles**	**V (mL)**	
MB#01	1	50	1	50	1	50	–	–	–	–
MB#02	1	50	1	50	1	50	–	1	12.5	–

Table 6
Materials inventory for palladium deposition during membrane preparation (referred to the selected functional unit).

Sample	Solutions required for palladium deposition (PD)								
	PD-1				PD-2				PD-3
	PD-1.1		PD-1.2		PD-2.1		PD-2.2		
	cycles	**V (mL)**	**cycles**	**V (mL)**	**cycles**	**V (mL)**	**cycles**	**V (mL)**	
MB#01	1	50	1	50	27 ± 3	200 ± 60	27 ± 3	81 ± 9	–
MB#02	1	50	1	50	12 ± 2	100 ± 40	12 ± 2	36 ± 6	–

consumptions were identical for the preparation of all the membranes, reaching a very similar modification of the original surface with an identical number of cycles.

A similar analysis has been presented in Table 6, where the solutions consumed for the palladium deposition (PD) are reported.

The support activation with Pd-nuclei (PD-1) always requires a constant volume of solutions PD-1.1 and PD-1.2 due to a unique cycle of 2 h generates enough Pd-seeds for the subsequent ELP-PP step in both membranes. However, a slight variation in the consumption of PD-2.1 and PD-2.2 solutions was observed during the preparation of the set of membranes, with 6 analogous samples of each type: MB#01 and MB#02. It could be attributed to the certainly heterogeneous surface of original supports and the possibility of certain differences between various raw supports. In fact, the greater modification of the original PSS substrates achieved after the incorporation of a ceramic intermediate barrier in MB#02 implies a noticeable reduction of the total number of ELP-PP recurrences in comparison to MB#01 in which only surface calcination of the original supports was carried out. In addition to this variation in the total number of ELP-PP recurrences due to the different surface properties of the supports, other causes can also provoke an increase in the spent volume of each solution. In fact, despite reusing the same solution for the entire set of recurrences in most cases, its degradation was also occasionally observed, thus turning in a dark orange-red color and being necessary its substitution by a fresh one. For this reason, errors collected in Table 6 could seem certainly high. This problem can be caused by diverse and unexpected operating issues, i.e. deviations in the control of temperature during the ELP-PP recurrences or direct contact between the solution and the metal assembling parts of the

deposition cell, normally covered by Teflon. Anyway, it should be noted that the probability of this occurrence is relatively low, avoiding taking into account these deviations for the present study. On the other hand, the final properties of all analogous composite-membranes were almost constant in terms of Pd-thickness, with an average deviation below 7%. Therefore, it can be assumed that the above-mentioned deviations do not affect the final quality of the membranes. Finally, as occurs during the surface modification, some washing and rinsing with distilled water were performed after both activation and ELP-PP recurrences, thus additionally consuming around 1400 ± 120 and 650 ± 80 mL during the fabrication of MB#01 and MB#02, respectively. These deviations of consumptions are caused by the above-mentioned necessity of additional ELP-PP recurrences in some cases.

3.3. Environmental performance: LCA results

LCA analysis of MB#01 is summarized in Fig. 5 as the relative contribution of each process stage in several environmental impacts. As it can be seen, the environmental impact is dominated by cleaning and drying step (PD-3), independently of the impact category selected. This result is directly related to the energy required to carry out the twenty-eight drying cycles (furnace at 110 °C for at least 8 h, each cycle) necessary to obtain a complete gas tightness using this procedure. At this point, it is necessary to point out one more time the lab-scale nature of the membrane synthesis procedure considered for the present study. The use of a more favorable production scale should minimize this contribution, replacing the electricity requirements of the electrical furnace with other alternatives well established in the industry. The high-energy consumption is also the reason that the SM-2 stage contributes around 15% to all the impact categories evaluated. It must be noticed that the electricity used in the studied process is assumed to be supplied by the Spanish electricity mix, having about 60% contribution of non-renewable resources. The incorporation of the fully dense Pd-film (PD-2) generates environmental impacts in all the selected categories due to the consumption of chemical products for the preparation of the required solutions, as well as their agitation. On the other hand, both the SM-1 and the PD-1 produce minimal environmental impacts, since they do not require the use of equipment with high electrical consumption, but only chemical reagents are used.

These results indicate that the environmental impacts associated with the production of MB#01 could be considerably reduced, improving the palladium deposition process, since it accounts for 80% of

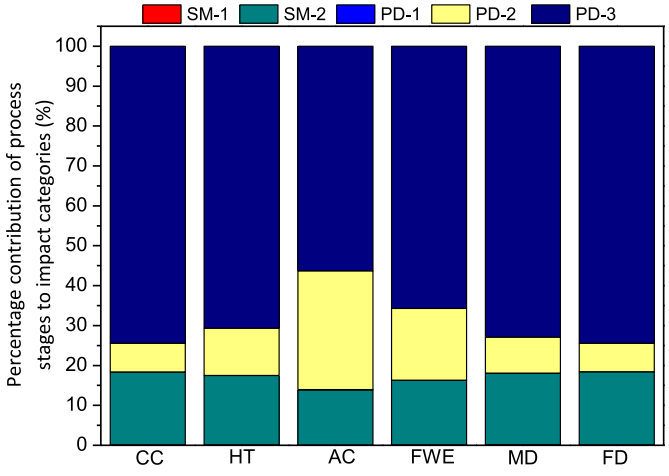

Fig. 5. LCA results for MB#01: percentage contribution of process stages to the evaluated impacts categories (CC: Climate Change; HT: Human Toxicity; AC: Acidification; FWE: Freshwater Ecotoxicity; MD: Metal Depletion; FD: fossil fuels depletion).

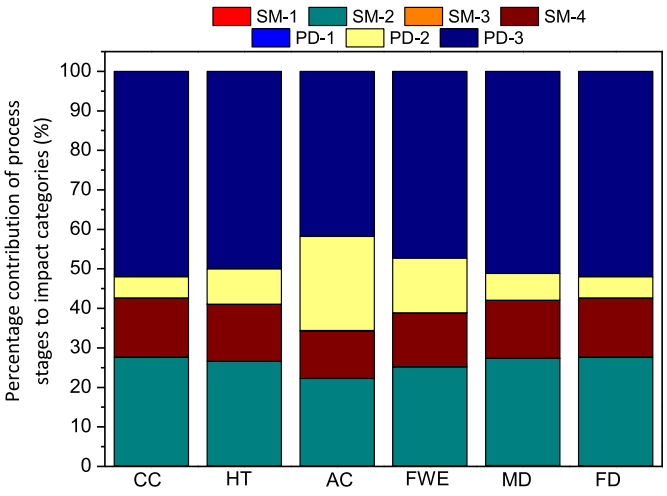

Fig. 6. LCA results for MB#02: percentage contribution of process stages to the evaluated impacts categories (CC: climate change; HT: human toxicity; AC: terrestrial acidification; FWE: freshwater ecotoxicity; MD: metal depletion; FD: fossil fuel depletion).

the total environmental impact. For this reason, the second method of membrane preparation called MB#02 has also been analyzed, to check whether the generation of an intermediate layer of CeO_2 before the deposition of palladium, allows reducing the environmental impact. The results for MB#02 are shown in Fig. 6.

Again, the stage with the greatest contribution to environmental impacts is PD-3, a stage in which the membrane is washed and dried before incorporating a new layer of palladium, although its impact has been reduced by an average of 20% in the selected categories regarding the MB#01 procedure. This is due to the lower number of cycles, thirteen in this procedure compared to twenty-eight in MB#01. Therefore, the electrical consumption has been remarkably reduced. This method MB#02, also favors the reduction of the impacts associated with plating (PD-2), specifically in the acidification and freshwater ecotoxicity categories because the number of chemical reagents necessary to carry out the deposition of palladium is less. The two additional stages of this method (SM-3 and SM-4) only contribute 15% to the environmental impact generated. This new impact generated is mainly due to the calcination of the support.

Comparing the LCA of the analyzed membranes (Table 7), an average reduction in the environmental impact of around 35% can be observed in the categories evaluated of the MB#02 as compared to MB#01. It can be seen that MB#02, despite being a synthesis procedure with a greater number of stages, to generate an intermediate layer of CeO_2 before palladium deposition, reduces the total environmental impact. Likewise, it should be noted that MB#02 improved its permeation behavior by around 350% compared to MB#01, generating a synergistic effect from an environmental point of view.

The purpose of this particular LCA on the preparation of ELP-PP

Table 7
Mid-point indicators of ReCiPe methodology of the different evaluated synthesis procedure (referred to the functional unit: one Pd-membrane with a length of 30 mm).

		MB#01	MB#02
ReCiPe indicators	Climate change (kg CO_{2eq})	7467.8	4962.4
	Human toxicity (kg 1,4-DCB)	630.5	413.9
	Terrestrial acidification (kg SO_{2eq})	26.1	16.3
	Freshwater ecotoxicity (kg 1,4-DCB)	9.4	6.1
	Metal depletion (kg Cu_{eq})	230.6	152.6
	Fossil fuel depletion (kg Oil_{eq})	2761.8	1835.4

membranes at laboratory scale is the identification of critical points in the synthesis route that could limit its eventual scale-up to a pilot or pre-industrial plant instead of concrete numerical results. Nevertheless, a Monte-Carlo analysis was carried out to estimate the uncertainties of laboratory data measurements, collecting all generated results in Fig. S2 as supplementary information. In summary, this analysis evidences that most of the impact categories are reduced for the synthesis strategy used with MB#02. Only natural land transformation, terrestrial ecotoxicity and water depletion reveal some doubts, becoming more relevant for the synthesis strategy used with MB#01 in some estimations. Nevertheless, most of the simulations predict lower environmental impacts also in these categories for MB#02 with percentages in the range 53–82%, always higher than 50%. Moreover, as previously addressed, the contribution of these particular categories was found almost residual in the present study. In this context, the particular results addressing the probability distribution function of selected impact categories in this study (CC, HT, AC, FEW, MD and FD) have been also included in Fig. S3 as supplementary information. For each case, the following statistical values have been displayed in the charts: mean, median and confidence limits at 2.5 and 97.5%. All these values could provide a first real indication about possible bottlenecks of the synthesis strategy carried out to obtain H_2-selective Pd-membranes by ELP-PP, being possible to

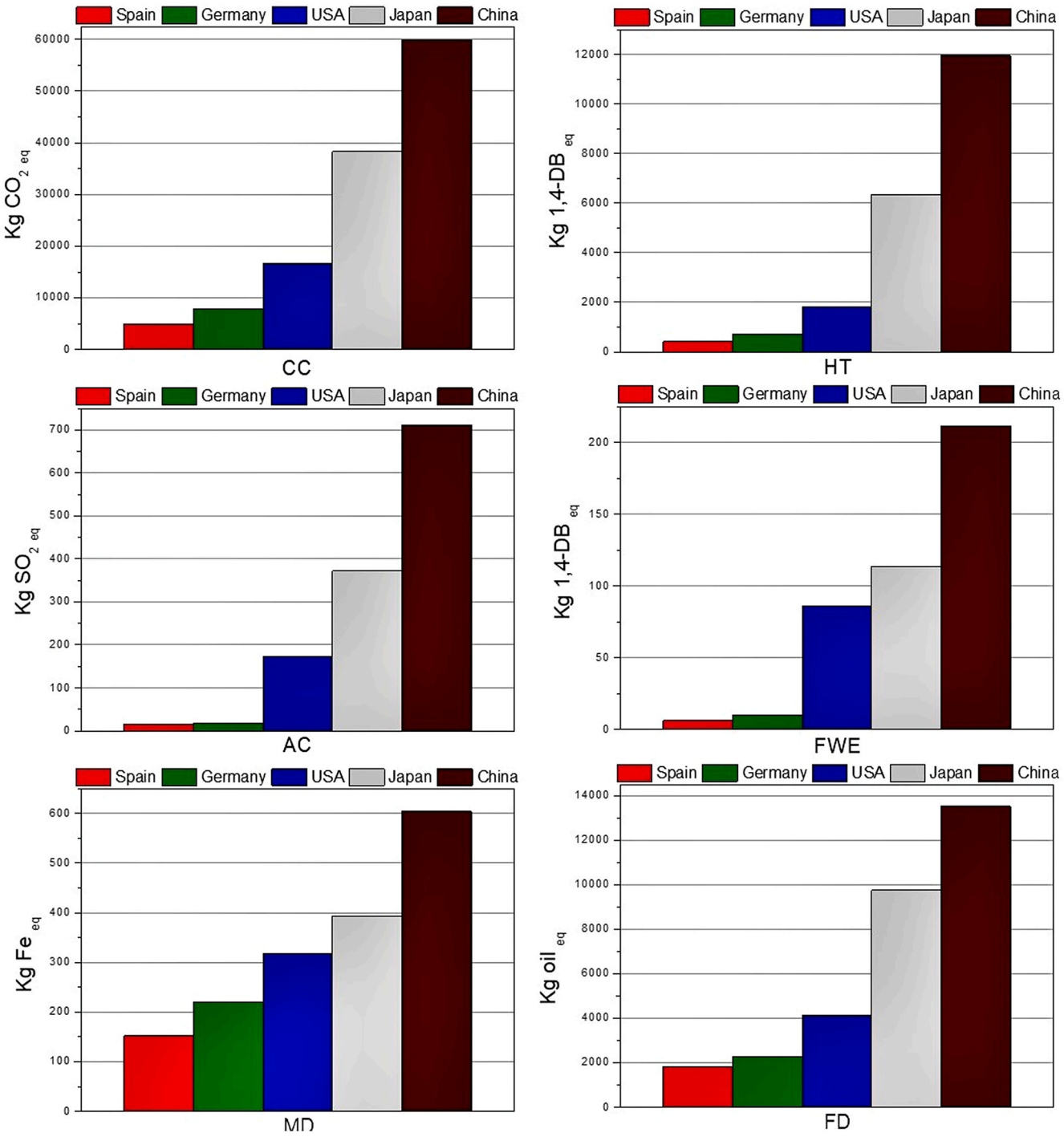

Fig. 7. LCA results for the preparation process of membrane MB#02 at lab-scale for different countries. Evaluated environmental impacts: Climate Change (CC), Human Toxicity (HT), Acidification (AC), Freshwater Ecotoxicity (FEW), Metal Depletion (MD) and Fossil-fuels Depletion (FD).

select the most adequate ones and apply the insights in other related fabrication techniques. Despite these insights could be also directly used as the basis for the prediction of possible environmental impacts at industrial scale, it is crucial to extend the study collecting experimental results at larger scales and conducting again the LCA. Moreover, the results should be discussed together with a complementary techno-economic assessment. This complete information will provide a well-rounded sustainability overview based on environmental and economical perspectives (van der Giesen et al., 2020).

3.4. Influence of electricity mix context

Proven the great influence generated by electricity consumption on the environmental impact referred to the functional unit. The specific energy production of each country was taken into account for a comparative objective, due to their different energy sources (Table 2). Fig. 7 shows LCA results for the MB#02 preparation process, at a laboratory scale for each country. In a general way, countries with a high contribution of renewable energies provide a more friendly manufacturing process of the functional unit. On the contrary, mix electricity production mainly based on fossil sources generates a higher environmental impact. Therefore, membrane preparation in countries with higher renewables sources can achieve a clean energy vector to a greater extent.

4. Conclusions

This study presents for the first time an analysis of the environmental impacts generated during the fabrication of composite Pd-membranes onto tubular porous stainless steel supports, being certainly innovative both preparation techniques and methodological choices at the basis of the assessment compared to the current state of the art. Two different strategies have been considered for the membrane preparation and compared, incorporating the H_2-selective palladium layer by Electroless Pore-Plating directly onto a calcined PSS support or after including an additional CeO_2 intermediate barrier. The secondary ceramic barrier allows reducing the required palladium amount to reach a fully dense membrane by 50%, while 350% higher H_2 permeances were obtained. Real data extracted from experiments at laboratory scale with a minimum uncertainty were considered for the life cycle inventory by considering one simple membrane with L = 30 mm and OD = 12.7 mm as functional unit. Among multiple possibilities, LCA analysis of both manufacturing processes through the ReCiPe methodology highlighted the most relevant environmental impacts (climate change, human toxicity, acidification, freshwater ecotoxicity, metal depletion, and fossil fuel resources depletion) and their main fabrication step contributions. Specifically, cleaning and drying is the most harmful stage (PD-3) due to the associated large electrical energy consumption. It can be overcome by incorporating CeO_2 intermediate layers, thus reducing the total required ELP-PP cycles and their associated cleaning and drying steps. In this manner, it is possible to reduce in 35% the environmental impact in most of the evaluated categories. These results were validated after considering the Monte-Carlo uncertainty analysis carried out, making crucial the location of the membrane production center and its particular electricity production system. It should be emphasized the nature of data used for the life cycle inventory, directly taken from experiments at laboratory scale for the fabrication of a tubular Pd-membrane with 30 mm in length. Despite the reproducibility of these values are verified for several membranes, the process scale-up for longer dimensions at pilot or pre-industrial scale could modify certain parameters, such as chemical solutions or electricity demands. Therefore, these preliminary results should be completed by analyzing in detail alternative fabrication processes for longer membranes. In this context, the current research provides a strong methodology to analyze rigorously the fabrication of Pd-composite membranes from an environmental point of view and combines the results with the membranes' performance to select the most adequate synthesis strategy. Thus, the use of CeO_2 intermediate barriers was found very attractive to reduce the environmental impacts generated during the membrane fabrication while simultaneously increasing the H_2 permeance. Future research on this topic is in progress, including the extension of the work for other alternative preparation strategies (i.e. doping the ceramic intermediate layer with Pd nuclei before the ELP-PP) and discussing the influence of membrane length on the generated environmental impacts. After completing the study, a wide knowledge about the fabrication of this type of membranes will allow selecting the most appropriate strategies to promote their penetration in the industry.

CRediT authorship contribution statement

D. Martinez-Diaz: Conceptualization, Methodology, Investigation, Formal analysis, Writing – original draft. **P. Leo:** Conceptualization, Methodology, Investigation, Formal analysis, Writing – original draft. **R. Sanz:** Supervision, Writing – review & editing. **A. Carrero:** Supervision, Writing – review & editing, Funding acquisition. **J.A. Calles:** Supervision, Writing – review & editing, Funding acquisition. **D. Alique:** Conceptualization, Methodology, Formal analysis, Resources, Writing – original draft, Writing – review & editing, Funding acquisition.

Declaration of competing interest

The authors declare that they have no known competing financial interests or personal relationships that could have appeared to influence the work reported in this paper.

Acknowledgments

The authors acknowledge the financial support achieved from the Spanish government through the competitive project ENE2017-83696-R and funds received from Young Researchers R&D Project Ref. M2182 - MEMRESPIP - financed by the Community of Madrid and Rey Juan Carlos University.

List of acronyms

AC	Acidification (environmental impact category)
AISI	American Iron and Steel Institute
CC	Climate change (environmental impact category)
CED	Cumulative Energy Deman
CHP	Combined Heat and Power
ELP	Electroless Plating
ELP-PP	Electroless Pore-Plating
FD	Fossil fuel depletion (environmental impact category)
FEW	Fresh water ecotoxicity (environmental impact category)
FU	Functional unit

HT	Human toxicity (environmental impact category)
ID	Inside Diameter (or internal diameter)
LCA	Life Cycle Assessment
LCI	Life Cycle Inventory
LCIA	Life Cycle Impact Assessment
MD	Metal depletion (environmental impact category)
OD	Outside Diameter (or external diameter)
PD	Palladium Deposition (membrane synthesis step)
PEM-FC	Proton-Exchange Membrane Fuel Cell
PSS	Porous Stainless Steel
PVA	Polyvynil-alcohol
SE	Secondary Electrons (for obtaining SEM images)
SEM	Scanning Electron Microscopy
SM	Support Modification (membrane synthesis step)
VA-DC	Vacuum-assisted dip-coating

List of symbols

$\alpha_{H2/N2}$	Ideal separation factor between hydrogen and nitrogen
E_a	Activation Energy (kJ mol^{-1})
J_{H2}	Hydrogen permeate (mol s^{-1})
L:	Membrane Length
P	Pressure (Pa)
$\mathscr{P}$	Hydrogen permeability (mol m^{-1} s^{-1} Pa$^{-0.5}$)
$\mathscr{P}^*$	Hydrogen permeance (mol m^{-2} s^{-1} Pa$^{-0.5}$)
$p_{H2,perm}$	Hydrogen partial pressure in the permeate side (Pa)
$p_{H2,ret}$:	Hydrogen partial pressure in the retentate side (Pa)
T	Temperature (°C)
t_{Pd}	Palladium thickness (μm)

Appendix A. Supplementary data

Supplementary data to this article can be found online at https://doi.org/10.1016/j.jclepro.2021.128229.

References

Abu-Rayash, A., Dincer, I., 2020. Analysis of the electricity demand trends amidst the COVID-19 coronavirus pandemic. Energy Res. Soc. Sci. 68, 101682. https://doi.org/10.1016/j.erss.2020.101682.

Aktar, M.A., Alam, M.M., Al-Amin, A.Q., 2021. Global economic crisis, energy use, CO2 emissions, and policy roadmap amid COVID-19. Sustain. Prod. Consum. 26, 770–781. https://doi.org/10.1016/j.spc.2020.12.029.

Alique, D., Imperatore, M., Sanz, R., Calles, J.A., Giacinti Baschetti, M., Baschetti, M.G., 2016. Hydrogen permeation in composite Pd-membranes prepared by conventional electroless plating and electroless pore-plating alternatives over ceramic and metallic supports. Int. J. Hydrogen Energy 41, 19430–19438. https://doi.org/10.1016/j.ijhydene.2016.06.128.

Alique, D., Martinez-Diaz, D., Sanz, R., Calles, J.A., 2018a. Review of supported pd-based membranes preparation by electroless plating for ultra-pure hydrogen production. https://doi.org/10.3390/membranes8010005.

Alique, D., 2018b. Processing and characterization of coating and thin film materials. In: Zhang, J., Jung, Y. (Eds.), Adv. Ceram. Met. Coat. Thin Film Mater. Energy Environ. https://doi.org/10.1007/978-3-319-59906-9.

Alique, D., Sanz, R., Calles, J.A., 2020. Pd membranes by electroless pore-plating: synthesis and permeation behavior. Curr. Trends Futur. Dev. Membr. 31–62. https://doi.org/10.1016/B978-0-12-818332-8.00002-8.

Anzelmo, B., Wilcox, J., Liguori, S., 2018. Hydrogen production via natural gas steam reforming in a Pd-Au membrane reactor. Comparison between methane and natural gas steam reforming reactions. J. Membr. Sci. 568 https://doi.org/10.1016/j.memsci.2018.09.054.

Arratibel, A., Medrano, J.A., Melendez, J., Pacheco Tanaka, D.A., van Sint Annaland, M., Gallucci, F., 2018a. Attrition-resistant membranes for fluidized-bed membrane reactors: double-skin membranes. J. Membr. Sci. 563, 419–426. https://doi.org/10.1016/j.memsci.2018.06.012.

Arratibel, A., Pacheco Tanaka, A., Laso, I., van Sint Annaland, M., Gallucci, F., 2018b. Development of Pd-based double-skinned membranes for hydrogen production in fluidized bed membrane reactors. J. Membr. Sci. 550, 536–544. https://doi.org/10.1016/J.MEMSCI, 2017.10.064.

Arratibel Plazaola, A., Pacheco Tanaka, D., Van Sint Annaland, M., Gallucci, F., Plazaola, A.A., Tanaka, D.A.P., Annaland, M.V.S., Gallucci, F., 2017. Recent advances in pd-based membranes for membrane reactors. Molecules 22, 1–53. https://doi.org/10.3390/molecules22010051.

Bare, J.C., Hofstetter, P., Pennington, D.W., Udo de Haes, H.A., 2000. Life cycle impact assessment workshop summary. Midpoints versus endpoints: the sacrifices and benefits. Int. J. Life Cycle Assess. 5, 319–326. https://doi.org/10.1007/BF02978665.

Baykara, S.Z., 2018. Hydrogen: a brief overview on its sources, production and environmental impact. Int. J. Hydrogen Energy 43, 10605–10614. https://doi.org/10.1016/j.ijhydene.2018.02.022.

Bdew, Energieversorgung, Die, 2020. 2020 – jahresbericht. https://www.bdew.de/media/documents/Jahresbericht_2020_20201218.pdf.

Bellini, S., Azzato, G., Caravella, A., 2020. Mass transport in hydrogen permeation through Pd-based membranes. Curr. Trends Futur. Dev. Membr 63–90. https://doi.org/10.1016/B978-0-12-818332-8.00003-X.

Bernardo, G., Araújo, T., da Silva Lopes, T., Sousa, J., Mendes, A., 2020. Recent advances in membrane technologies for hydrogen purification. Int. J. Hydrogen Energy. https://doi.org/10.1016/j.ijhydene.2019.06.162.

Bottino, A., Broglia, M., Capannelli, G., Comite, A., Pinacci, P., Scrignari, M., Azzurri, F., 2014. Sol–gel synthesis of thin alumina layers on porous stainless steel supports for high temperature palladium membranes. Int. J. Hydrogen Energy 39, 4717–4724. https://doi.org/10.1016/j.ijhydene.2013.11.096.

Brunetti, A., Caravella, A., Drioli, E., Barbieri, G., 2017. Chapter 1. Membr. Reactors Hydrogen Prod. 2, 1–29. https://doi.org/10.1039/9781788010443-00001.

Cai, Y., Sam, C.Y., Chang, T., 2018. Nexus between clean energy consumption, economic growth and CO2 emissions. J. Clean. Prod. 182, 1001–1011. https://doi.org/10.1016/J.JCLEPRO, 2018.02.035.

Calles, J.A., Sanz, R., Alique, D., Furones, L., 2014. Thermal stability and effect of typical water gas shift reactant composition on {H2} permeability through a Pd-YSZ-PSS composite membrane. Int. J. Hydrogen Energy 39, 1398–1409. https://doi.org/10.1016/j.ijhydene.2013.10.168.

Calles, J.A., Sanz, R., Alique, D., Furones, L., Marín, P., Ordoñez, S., 2018. Influence of the selective layer morphology on the permeation properties for Pd-PSS composite membranes prepared by electroless pore-plating: experimental and modeling study. Separ. Purif. Technol. 194, 10–18. https://doi.org/10.1016/j.seppur.2017.11.014.

Cao, Z., Jiang, H., Luo, H., Baumann, S., Meulenberg, W.A., Voss, H., Caro, J., 2012. Simultaneous overcome of the equilibrium limitations in BSCF oxygen-permeable membrane reactors: water splitting and methane coupling. Catal. Today 193, 2–7. https://doi.org/10.1016/j.cattod.2011.12.018.

Caravella, A., Hara, S., Drioli, E., Barbieri, G., 2013. Sieverts law pressure exponent for hydrogen permeation through Pd-based membranes: coupled influence of non-ideal diffusion and multicomponent external mass transfer. Int. J. Hydrogen Energy 38, 16229–16244. https://doi.org/10.1016/j.ijhydene.2013.09.102.

Chen, P.-Y., Chen, S.-T., Hsu, C.-S., Chen, C.-C., 2016. Modeling the global relationships among economic growth, energy consumption and CO2 emissions. Renew. Sustain. Energy Rev. 65, 420–431. https://doi.org/10.1016/J.RSER, 2016.06.074.

Choi, D.H., Chun, S.M., Ma, S.H., Hong, Y.C., 2016. Production of hydrogen-rich syngas from methane reforming by steam microwave plasma. J. Ind. Eng. Chem. 34, 286–291. https://doi.org/10.1016/j.jiec.2015.11.019.

Conde, J.J., Maroño, M., Sánchez-Hervás, J.M., 2017. Pd-based membranes for hydrogen separation: review of alloying elements and their influence on membrane properties. Separ. Purif. Rev. 46, 152–177. https://doi.org/10.1080/15422119.2016.1212379.

Corpus-Mendoza, A.N., Ruiz-Segoviano, H.S., Rodríguez-Contreras, S.F., Yañez-Dávila, D., Hernández-Granados, A., 2021. Decrease of mobility, electricity demand, and NO2 emissions on COVID-19 times and their feedback on prevention measures. Sci. Total Environ. 760, 143382. https://doi.org/10.1016/j.scitotenv.2020.143382.

Coutanceau, C., Baranton, S., Audichon, T., 2018. Chapter 2-hydrogen production from thermal reforming BT - hydrogen electrochemical production. In: Hydrog. Energy Fuel Cells Prim. Academic Press, pp. 7–15. https://doi.org/10.1016/B978-0-12-811250-2.00002-9.

Detchusananard, T., Im-orb, K., Ponpesh, P., Arpornwichanop, A., 2018. Biomass gasification integrated with CO2 capture processes for high-purity hydrogen production: process performance and energy analysis. Energy Convers. Manag. 171, 1560–1572. https://doi.org/10.1016/j.enconman.2018.06.072.

Di Marcoberardino, G., Binotti, M., Manzolini, G., Viviente, J.L., Arratibel, A., Roses, L., Gallucci, F., 2017. Achievements of European projects on membrane reactor for hydrogen production. J. Clean. Prod. 161, 1442–1450. https://doi.org/10.1016/j.jclepro.2017.05.122.

Dogan, M., Kilicarslan, S., 2008. Effects of process parameters on the synthesis of palladium membranes. Nucl. Instrum. Methods Phys. Res. Sect. B Beam Interact. Mater. Atoms 266, 3458–3466. https://doi.org/10.1016/j.nimb.2008.05.011.

EIA, Short-Term, 2020. Energy outlook (STEO) forecast highlights. US EIA - Short-Term Energy Outlook 1–53. https://www.eia.gov/outlooks/steo/report/electricity.php.

Finkbeiner, M., Inaba, A., Tan, R.B.H., Christiansen, K., Klüppel, H.-J., 2006. The new international standards for life cycle assessment. Int. J. Life Cycle Assess. 11, 80–85. https://doi.org/10.1065/lca2006.02.002.

Furlan, C., Mortarino, C., 2018. Forecasting the impact of renewable energies in competition with non-renewable sources. Renew. Sustain. Energy Rev. 81, 1879–1886. https://doi.org/10.1016/j.rser.2017.05.284.

Furones, L., Alique, D., 2017. Interlayer properties of in-situ oxidized porous stainless steel for preparation of composite Pd membranes. ChemEngineering 2, 1. https://doi.org/10.3390/chemengineering2010001.

Gallucci, F., Fernandez, E., Corengia, P., van Sint Annaland, M., 2013. Recent advances on membranes and membrane reactors for hydrogen production. Chem. Eng. Sci. 92, 40–66. https://doi.org/10.1016/j.ces.2013.01.008.

Guo, Y., Wu, H., Jin, Y., Zhou, L., Chen, Q., Fan, X., 2017. Deposition of TS-1 zeolite film on palladium membrane for enhancement of membrane stability. Int. J. Hydrogen Energy 42, 27111–27121. https://doi.org/10.1016/j.ijhydene.2017.09.127.

Han, J.-Y., Kim, C.-H., Lim, H., Lee, K.-Y., Ryi, S.-K., 2017. Diffusion barrier coating using a newly developed blowing coating method for a thermally stable Pd membrane deposited on porous stainless-steel support. Int. J. Hydrogen Energy 42, 12310–12319. https://doi.org/10.1016/j.ijhydene.2017.03.053.

Hatlevik, Ø., Gade, S.K., Keeling, M.K., Thoen, P.M., Davidson, A.P.P., Way, J.D., 2010. Palladium and palladium alloy membranes for hydrogen separation and production: history, fabrication strategies, and current performance. Separ. Purif. Technol. 73, 59–64. https://doi.org/10.1016/j.seppur.2009.10.020.

Huang, Y., Dittmeyer, R., 2007. Preparation of thin palladium membranes on a porous support with rough surface. J. Membr. Sci. 302, 160–170. https://doi.org/10.1016/j.memsci.2007.06.040.

Huang, Y., Liu, Q., Jin, X., Ding, W., Hu, X., Li, H., 2020. Coating the porous Al2O3 substrate with a natural mineral of Nontronite-15A for fabrication of hydrogen-permeable palladium membranes. Int. J. Hydrogen Energy 45, 7412–7422. https://doi.org/10.1016/j.ijhydene.2019.04.102.

Huijbregts, M.A.J., Hellweg, S., Frischknecht, R., Hendriks, H.W.M., Hungerbühler, K., Hendriks, A.J., 2010. Cumulative energy demand as predictor for the environmental burden of commodity production. Environ. Sci. Technol. 44, 2189–2196. https://doi.org/10.1021/es902870s.

Huijbregts, M.A.J., Steinmann, Z.J.N., Elshout, P.M.F., Stam, G., Verones, F., Vieira, M., Zijp, M., Hollander, A., van Zelm, R., 2017. ReCiPe2016: a harmonised life cycle impact assessment method at midpoint and endpoint level. Int. J. Life Cycle Assess. 22, 138–147. https://doi.org/10.1007/s11367-016-1246-y.

Igos, E., Rugani, B., Rege, S., Benetto, E., Drouet, L., Zachary, D.S., 2015. Combination of equilibrium models and hybrid life cycle-input-output analysis to predict the environmental impacts of energy policy scenarios. Appl. Energy 145, 234–245. https://doi.org/10.1016/j.apenergy.2015.02.007.

Iulianelli, A., Jansen, J.C., Esposito, E., Longo, M., Dalena, F., Basile, A., 2019. Hydrogen permeation and separation characteristics of a thin Pd-Au/Al 2 O 3 membrane: the effect of the intermediate layer absence. Catal. Today 330, 32–38. https://doi.org/10.1016/j.cattod.2018.04.029.

Jiang, P., Van Fan, Y., Klemeš, J.J., 2021. Impacts of COVID-19 on energy demand and consumption: challenges, lessons and emerging opportunities. Appl. Energy 285. https://doi.org/10.1016/j.apenergy.2021.116441.

Kakoulaki, G., Kougias, I., Taylor, N., Dolci, F., Moya, J., Jäger-Waldau, A., 2021. Green hydrogen in Europe – a regional assessment: substituting existing production with electrolysis powered by renewables. Energy Convers. Manag. 228 https://doi.org/10.1016/j.enconman.2020.113649.

Karagöz, S., Tsotsis, T.T., Manousiouthakis, V.I., 2020. Multi-scale model based design of membrane reactor/separator processes for intensified hydrogen production through the water gas shift reaction. Int. J. Hydrogen Energy. https://doi.org/10.1016/j.ijhydene.2019.05.118.

Kim, C.-H., Han, J.-Y., Lim, H., Lee, K.-Y., Ryi, S.-K., 2017. Methane steam reforming using a membrane reactor equipped with a Pd-based composite membrane for effective hydrogen production. Int. J. Hydrogen Energy. https://doi.org/10.1016/j.ijhydene.2017.10.054.

Kim, C.H., Han, J.Y., Kim, S., Lee, B., Lim, H., Lee, K.Y., Ryi, S.K., 2018. Hydrogen production by steam methane reforming in a membrane reactor equipped with a Pd composite membrane deposited on a porous stainless steel. Int. J. Hydrogen Energy 43, 7684–7692. https://doi.org/10.1016/j.ijhydene.2017.11.176.

Liguori, S., Kian, K., Buggy, N., Anzelmo, B.H., Wilcox, J., 2020. Opportunities and challenges of low-carbon hydrogen via metallic membranes. Prog. Energy Combust. Sci. 80, 100851. https://doi.org/10.1016/j.pecs.2020.100851.

Lux, B., Pfluger, B., 2020. A supply curve of electricity-based hydrogen in a decarbonized European energy system in 2050,. Appl. Energy 269, 115011. https://doi.org/10.1016/j.apenergy.2020.115011.

Mallory, G.O., Hajdu, J.B., 1990. Electroless plating: fundamentals and applications. Am. Electropl. Surf. Finishers Soc.

Maroño, M., Dacute, G., Alessandro, Morales, A., Martinez-Diaz, D., Alique, D., Sánchez, J.M., 2020. Influence of Si and Fe/Cr oxides as intermediate layers in the fabrication of supported Pd membranes. Separ. Purif. Technol. 234 https://doi.org/10.1016/j.seppur.2019.116091.

Martinez-Diaz, D., Sanz, R., Calles, J.A., Alique, D., 2019. H2 permeation increase of electroless pore-plated Pd/PSS membranes with CeO2 intermediate barriers, Sep. Purif. Technol. 216, 16–24. https://doi.org/10.1016/J.SEPPUR, 2019.01.076.

Martinez-Diaz, D., Alique, D., Calles, J.A.A., Sanz, R., 2020. Pd-thickness reduction in electroless pore-plated membranes by using doped-ceria as interlayer. Int. J. Hydrogen Energy 45, 7278–7289. https://doi.org/10.1016/j.ijhydene.2019.10.140.

Martinez-Diaz, D., Martínez del Monte, D., García-Rojas, E., Alique, D., Calles, J.A., Sanz, R., 2021. Comprehensive permeation analysis and mechanical resistance of electroless pore-plated Pd-membranes with ordered mesoporous ceria as intermediate layer. Separ. Purif. Technol. 258, 118066. https://doi.org/10.1016/j.seppur.2020.118066.

Mateos-Pedrero, C., Soria, M.A., Rodríguez-Ramos, I., Guerrero-Ruiz, A., 2010. Modifications of porous stainless steel previous to the synthesis of Pd membranes. In: Stud. Surf. Sci. Catal, pp. 779–783. https://doi.org/10.1016/S0167-2991(10)75159-4.

Melendez, J., Fernandez, E., Gallucci, F., van Sint Annaland, M., Arias, P.L., Pacheco Tanaka, D.A., Tanaka, D.A.P., 2017. Preparation and characterization of ceramic supported ultra-thin (~1 μm) Pd-Ag membranes. J. Membr. Sci. 528, 12–23. https://doi.org/10.1016/j.memsci.2017.01.011.

Mivechian, A., Pakizeh, M., 2013. Performance comparison of different separation systems for H2 recovery from catalytic reforming unit off-gas streams. Chem. Eng. Technol. 36, 519–527. https://doi.org/10.1002/ceat.201200558.

Muradov, N.Z., 2008. T.N. Veziroğlu, "Green" path from fossil-based to hydrogen economy: an overview of carbon-neutral technologies. Int. J. Hydrogen Energy 33, 6804–6839. https://doi.org/10.1016/j.ijhydene.2008.08.054.

Navajas, A., Mittal, N., Rangnekar, N., Zhang, H., Cornejo, A., Gandía, L.M., Tsapatsis, M., 2018. Environmental evaluation of the improvements for industrial scaling of zeolite membrane manufacturing by life cycle assessment. ACS Sustain. Chem. Eng. 6, 15773–15780. https://doi.org/10.1021/acssuschemeng.8b04336.

Nikolaidis, P., Poullikkas, A., 2017. A comparative overview of hydrogen production processes. Renew. Sustain. Energy Rev. 67, 597–611. https://doi.org/10.1016/j.rser.2016.09.044.

Ozawa, A., Kudoh, Y., Murata, A., Honda, T., Saita, I., Takagi, H., 2018. Hydrogen in low-carbon energy systems in Japan by 2050: the uncertainties of technology development and implementation. Int. J. Hydrogen Energy 43, 18083–18094. https://doi.org/10.1016/j.ijhydene.2018.08.098.

Pambudi, N.A., Itaoka, K., Kurosawa, A., Yamakawa, N., 2017. Impact of hydrogen fuel for CO2 emission reduction in power generation sector in Japan. Energy Procedia 105, 3075–3082. https://doi.org/10.1016/j.egypro.2017.03.642.

Parra, D., Valverde, L., Pino, F.J., Patel, M.K., 2019. A review on the role, cost and value of hydrogen energy systems for deep decarbonisation, Renew. Sustain. Energy Rev. 101, 279–294. https://doi.org/10.1016/J.RSER, 2018.11.010.

Peters, T.A., Carvalho, P.A., van Wees, J.F., Overbeek, J.P., Sagvolden, E., van Berkel, F. P.F., Løvvik, O.M., Bredesen, R., 2018. Leakage evolution and atomic-scale changes in Pd-based membranes induced by long-term hydrogen permeation. J. Membr. Sci. 563, 398–404. https://doi.org/10.1016/j.memsci.2018.06.008.

Prézélus, F., Tiruta-Barna, L., Guigui, C., Remigy, J.C., 2021. A generic process modelling – LCA approach for UF membrane fabrication: application to cellulose acetate membranes. J. Membr. Sci. 618 https://doi.org/10.1016/j.memsci.2020.118594.

Ryi, S.-K., Ahn, H.-S., Park, J.-S., Kim, D.-W., 2014. Pd–Cu alloy membrane deposited on CeO2 modified porous nickel support for hydrogen separation. Int. J. Hydrogen Energy 39, 4698–4703. https://doi.org/10.1016/j.ijhydene.2013.11.031.

Saeedmanesh, A., Mac Kinnon, M.A., Brouwer, J., 2018. Hydrogen is essential for sustainability. Curr. Opin. Electrochem. 12, 166–181. https://doi.org/10.1016/j.coelec.2018.11.009.

Sanz, R., Calles, J.A., Alique, D., Furones, L., Ordóñez, S., Marín, P., Corengia, P., Fernandez, E., 2011. Preparation, testing and modelling of a hydrogen selective Pd/YSZ/SS composite membrane. Int. J. Hydrogen Energy 36, 15783–15793. https://doi.org/10.1016/j.ijhydene.2011.08.102.

Sanz, R., Calles, J.A., Alique, D., Furones, L., 2012. New synthesis method of Pd membranes over tubular {PSS} supports via "pore-plating" for hydrogen separation processes. Int. J. Hydrogen Energy 37, 18476–18485. https://doi.org/10.1016/j.ijhydene.2012.09.084.

Sholl, R.P., 2016. D.S.; Lively, Seven chemical separation to change the world. Nature 532, 435–437.
Simonen, K., 2014. Life cycle assessment. Life Cycle Assess 1–159. https://doi.org/10.4324/9781315778730.
Sistema, E.L., Informe, 2019. 2019 Red Electrica Española.
Souleimanova, R.S., Mukasyan, A.S., Varma, A., 2000. Effects of osmosis on microstructure of Pd-composite membranes synthesized by electroless plating technique. J. Membr. Sci. 166, 249–257. https://doi.org/10.1016/S0376-7388(99)00268-9.
Sovacool, B.K., Furszyfer Del Rio, D., Griffiths, S., 2020. Contextualizing the Covid-19 pandemic for a carbon-constrained world: insights for sustainability transitions, energy justice, and research methodology. Energy Res. Soc. Sci. 68, 101701. https://doi.org/10.1016/j.erss.2020.101701.
Szulejko, J.E., Kumar, P., Deep, A., Kim, K.-H., 2017. Global warming projections to 2100 using simple CO2 greenhouse gas modeling and comments on CO2 climate sensitivity factor. Atmos. Pollut. Res. 8, 136–140. https://doi.org/10.1016/J.APR, 2016.08.002.
Tarditi, A.M., Bosko, M.L., Cornaglia, L.M., 2017. In: Electroless Plating of Pd Binary and Ternary Alloys and Surface Characteristics for Application in Hidrogen Separation. Elsevier, Oxford, pp. 1–24. https://doi.org/10.1016/B978-0-12-803581-8.09166-9.
Tosto, E., Alique, D., Martinez-Diaz, D., Sanz, R., Calles, J.A.A., Caravella, A., Medrano, J.A.A., Gallucci, F., 2020. Stability of pore-plated membranes for hydrogen production in fluidized-bed membrane reactors. Int. J. Hydrogen Energy 45, 7374–7385. https://doi.org/10.1016/j.ijhydene.2019.04.285.
Turconi, R., Boldrin, A., Astrup, T., 2013. Life cycle assessment (LCA) of electricity generation technologies: overview, comparability and limitations. Renew. Sustain. Energy Rev. 28, 555–565. https://doi.org/10.1016/j.rser.2013.08.013.
US Energy Information Administration EIA, 2020. Country analysis executive summary: China. https://www.eia.gov/international/content/analysis/countries_long/China/china.pdf, 9.
Vadrucci, M., Borgognoni, F., Moriani, A., Santucci, A., Tosti, S., 2013. Hydrogen permeation through Pd–Ag membranes: surface effects and Sieverts' law. Int. J. Hydrogen Energy 38, 4144–4152. https://doi.org/10.1016/j.ijhydene.2013.01.091.
Valente, A., Iribarren, D., Dufour, J., 2017. Life cycle assessment of hydrogen energy systems: a review of methodological choices. Int. J. Life Cycle Assess. 22, 346–363. https://doi.org/10.1007/s11367-016-1156-z.
van der Giesen, C., Cucurachi, S., Guinée, J., Kramer, G.J., Tukker, A., 2020. A critical view on the current application of LCA for new technologies and recommendations for improved practice. J. Clean. Prod. 259 https://doi.org/10.1016/j.jclepro.2020.120904.
Voss, C., 2005. Applications of pressure swing adsorption technology. Adsorption 11, 527–529. https://doi.org/10.1007/s10450-005-5979-3.
Wernet, G., Bauer, C., Steubing, B., Reinhard, J., Moreno-Ruiz, E., Weidema, B., 2016. The ecoinvent database version 3 (part I): overview and methodology. Int. J. Life Cycle Assess. 21, 1218–1230. https://doi.org/10.1007/s11367-016-1087-8.
Wim Elseviers, M.W., Hassett, Paula Flowers, Navarre, Jean-Louis, 2015. 50 Years of PSA technology for H2 purification, UOP. https://www.uop.com/?document=psa-50-paper&download=1.
Yanagisawa, A., Ikarii, R., Iwata, S., Hwang, I.H., Tomokawa, K., Shibata, Y., Ito, K., 2014. Economic and energy outlook of Japan for FY2015. http://eneken.ieej.or.jp/data/5903.pdf, 1-28.
Yepes, D., Cornaglia, L.M., Irusta, S., Lombardo, E.A., 2006. Different oxides used as diffusion barriers in composite hydrogen permeable membranes. J. Membr. Sci. 274, 92–101. https://doi.org/10.1016/j.memsci.2005.08.003.
Yin, H., Yip, A.C.K., 2017. A review on the production and purification of biomass-derived hydrogen using emerging membrane technologies. Catal. 7 https://doi.org/10.3390/catal7100297.
Yue, X.-L., Gao, Q.-X., 2018. Contributions of natural systems and human activity to greenhouse gas emissions. Adv. Clim. Change Res. 9, 243–252. https://doi.org/10.1016/J.ACCRE, 2018.12.003.
Yun, S., Ted Oyama, S., Oyama, S.T., 2011. Correlations in palladium membranes for hydrogen separation: a review. J. Membr. Sci. 375, 28–45. https://doi.org/10.1016/j.memsci.2011.03.057.
Zhao, C., Caravella, A., Xu, H., Brunetti, A., Barbieri, G., Goldbach, A., 2018a. Support mass transfer resistance of Pd/ceramic composite membranes in the presence of sweep gas. J. Membr. Sci. 550 https://doi.org/10.1016/j.memsci.2017.12.082.
Zhao, C., Xu, H., Goldbach, A., 2018b. Duplex Pd/ceramic/Pd composite membrane for sweep gas-enhanced CO2 capture. J. Membr. Sci. 563, 388–397. https://doi.org/10.1016/J.MEMSCI, 2018.05.057.
Zheng, L., Li, H., Xu, H., 2016. "Defect-free" interlayer with a smooth surface and controlled pore-mouth size for thin and thermally stable Pd composite membranes. Int. J. Hydrogen Energy 41, 1002–1009. https://doi.org/10.1016/j.ijhydene.2015.09.024.
Zornoza, B., Casado, C., Navajas, A., 2013. Chapter 11-advances in hydrogen separation and purification with membrane technology. In: Gandía, L.M., Arzamendi, G., Diéguez, P.M. (Eds.), Renew. Hydrog. Technol. Elsevier, Amsterdam, pp. 245–268. https://doi.org/10.1016/B978-0-444-56352-1.00011-8.